ACS Sustainable Chemistry & Engineering

Research Article

pubs.acs.org/journal/ascecg

Pyrene-Based Porous Organic Polymers as Efficient Catalytic Support for the Synthesis of Biodiesels at Room Temperature

Sudipta K. Kundu and Asim Bhaumik*

Department of Materials Science, Indian Association for the Cultivation of Science, Jadavpur, Kolkata-700032, India

Supporting Information

ABSTRACT: New pyrene-based microporous organic polymers PPOP-1, PPOP-2, and PPOP-3 have been synthesized via Friedel–Crafts alkylation reaction between pyrene and bis(1,4-dibromomethyl)benzene at their different molar ratios in the presence of a Lewis acid catalyst $FeCl_3$ under refluxing conditions. Pore surfaces of PPOP-1, PPOP-2, and PPOP-3 have been functionalized by $-SO_3H$ groups via chlorosulfonic acid treatment under controlled reaction conditions to obtain sulfonated porous organic polymers, and these are designated as SPPOP-1, SPPOP-2, and SPPOP-3, respectively. Powder X-ray diffraction, N_2 sorption, HR-TEM, FE-SEM, NH_3-TPD, solid state ^{13}C CP MAS-NMR, and FT-IR spectroscopic tools are employed to characterize these materials. These sulfonated porous polymers showed nanofiber-like or spherical morphology, very high surface acidity, and excellent catalytic activity for the synthesis of biodiesels via esterification/transesterification of long chain fatty acids/esters at room temperature together with very high recycling efficiency, suggesting the future potential of these sulfonated porous polymers in a wide range of sustainable acid-catalyzed chemical reactions.

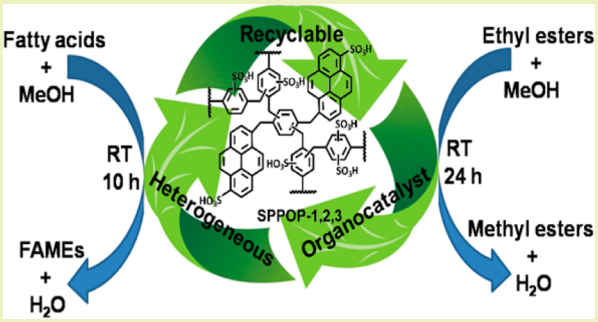

KEYWORDS: *Biodiesel, Esterification/trans-esterification reaction, Porous organic polymer, Sulfonation, Surface acidity*

INTRODUCTION

Biodiesel is increasingly becoming a popular alternative to fossil fuels due to the worldwide energy crisis, demand for the conservation of nonrenewable natural resources, and increasing price of petroleum-based diesel fuels together with environmenta; concerns caused by the combustion of fossil fuels.[1] Fatty acid methyl or ethyl esters (FAMEs or FAEEs) show great potential as diesel substitutes, and they are sustainable, sulfur-free, biodegradable, nontoxic diesel fuel substitutes that are widely used worldwide.[2,3] Biodiesel is a low-emissions diesel substitute fuel and can be easily produced either through transesterification of triglycerides or the esterification of free fatty acids (FFAs) with short-chained alcohols, mainly methanol in the presence of suitable acid or base catalysts.[4,5] One of the most common ways to produce biodiesel is through transesterification, especially alkali-catalyzed transesterification of vegetable oils.[6] However, the process requires efficient wastewater management to make it industrially viable.[7] On the other hand, if feedstock with a high level of free fatty acid (FFA) is used (soapstock, recycled oils, greases, cooking oils, etc.), the acid-catalyzed esterification with methanol or glycerol prior to transesterification is more desirable.[8,9] In this context, it is pertinent to mention that the industrial production of esters via esterification and transesterification reactions in the presence of homogeneous acid catalysts such as H_2SO_4[10] or H_3PO_4[11] require high temperature, expensive equipment, product separation, and purification and faces a problem with nonreusability of the catalysts.[12] Moreover, these mineral acids are corrosive in nature, and they have to be neutralized after the reaction. On the other hand, conventional base catalysts such as NaOH and KOH catalyze both esterification and transesterification reactions, but the workup of the reaction requires a lot of water to wash out the byproduct soap.[7] This requirement makes these catalysts environmentally unfriendly. Due to formation of soap, the use of conventional base catalysts such as alkali metal hydroxides and alkoxides[13−17] faces saponification and product separation problems. This problem can be solved by performing a two-step process. The first is the esterification of FFAs to alkyl ester in the presence of an acid catalyst followed by the second step of transesterification using a base catalyst.[18]

More recently, a green approach for biodiesel production via sustainable heterogeneous acid catalysts has attracted significant attraction vis-à-vis conventional hazardous and corrosive homogeneous acid catalysts, as the materials of the former category are environmentally friendly, reusable, and easily separable from the reaction mixture.[19−30] In spite of nontoxicity and reusability, these solid acid catalysts should have high stability, numerous strong acid sites, high surface area, and low cost. The most acid catalysts reported so far are expensive or involve complex synthetic procedures during their preparation. These include sulfated zirconia,[19] tungstated zirconia,[20] sulfated

Received: March 25, 2015
Revised: June 19, 2015
Published: June 29, 2015

DOI: 10.1021/acssuschemeng.5b00238
ACS Sustainable Chem. Eng. 2015, 3, 1715−1723

tin oxide,[21] sulfonated carbon,[22,23] mesoporous metarials,[24] ion-exchange resin,[25] nafion-based composites[26] sulfonated incompletely carbonized sugar, starch, or cellulose.[27−30] In recent years, porous heterogeneous acid catalysts such as zirconium oxophosphates,[31] metal organic framework (MOF) encapsulated Keggin heteropolyacid,[32] and sulfonic acid functionalized hybrid silica[33] have been extensively studied for the esterification reactions. But in most of these cases, the reactions are also carried out at moderately high temperature. There are very few reports on the synthesis of biodiesel products at room temperature.[34]

In this context, it is pertinent to mention that in recent years considerable attention has been paid to the design and synthesis of porous organic materials, which bear reactive organic functional groups at the pore surface together with high surface area. Apart from offering highly reactive functional groups exposed to the pore surface, these soft porous materials are particularly demanding as green organocatalysts due to being devoid of toxic metals. These organically functionalized porous materials are employed in various frontline applications like separation,[35−41] adsorption,[42−45] gas storage,[46−48] supercapacitors,[49] sensing,[50−52] and heterogeneous catalysis.[53−58] Recently, we have developed a sulfonated carbazole-based hyper-cross-linked supermicroporous polymer for the synthesis of biodiesel at room temperature.[59] The carbazole-based polymer is synthesized by Friedel−Crafts alkylation using $FeCl_3$ as the Lewis acid catalyst, and it has been functionalized by $-SO_3H$ groups. Due to presence of N-sites in the polymer network, a small amount of iron is bounded in the polymer network, which could interfere with the catalytic reactions. Further, the conversion of soybean oil over this sulfonated polymer is also low. Thus, from the perspective of green and sustainable synthesis, it is highly desirable to design a new porous metal-free heterogeneous organocatalyst for the successful and economical production of biodiesels in high yields at room temperature.

Herein, we first report the sulfonic acid functionalized porous organic polymers SPPOP-1, SPPOP-2, and SPPOP-3 via sulfonation of respective pyrene-based porous organic polymers synthesized through a Friedel−Crafts alkylation reaction between different molar ratios of bis(1,4-bromomethyl)-benzene and pyrene (Scheme 1). Functionalization of these porous polymers with sulfonic acid groups on the aromatic rings by chlorosulfonic acid leads to the formation of microporous organocatalysts with a high BET surface area together with a large amount of surface $-SO_3H$ groups. Both parent polymers and sulfonated materials were thoroughly characterized by using powder XRD, N_2 sorption, HR-TEM, FE-SEM, FT-IR, TG-DTA, NH_3-TPD, UV−vis, etc. and were successfully employed for the synthesis of biofuels under eco-friendly reaction conditions.

EXPERIMENTAL SECTION

Synthesis of Pyrene-Based Covalent Organic Polymers. In a typical reaction, 0.105 g (0.4 mmol) of bis(1,4-bromomethyl)benzene and 0.04 g (0.2 mmol) of pyrene were dissolved in 8 mL anhydrous 1,2-dichloroethane. A total of 0.2 g anhydrous ferric chloride was added into the above mixture with occasional shaking and maintaining the reaction temperature of 20−25 °C. Then the mixture was refluxed at 80 °C for 20 h. The precipitated solid was filtered and washed with methanol until the filtrate did not give a deep blue color upon addition of potassium ferrocyanide. The precipitate was extracted by refluxing with methanol in a Soxhlet apparatus for 2 days and dried under vacuum at 60 °C. This polymer is designated as PPOP-1. Similarly,

Scheme 1. Sulfonic Acid Functionalized Porous Organic Polymers SPPOP-1, SPPOP-2, and SPPOP-3

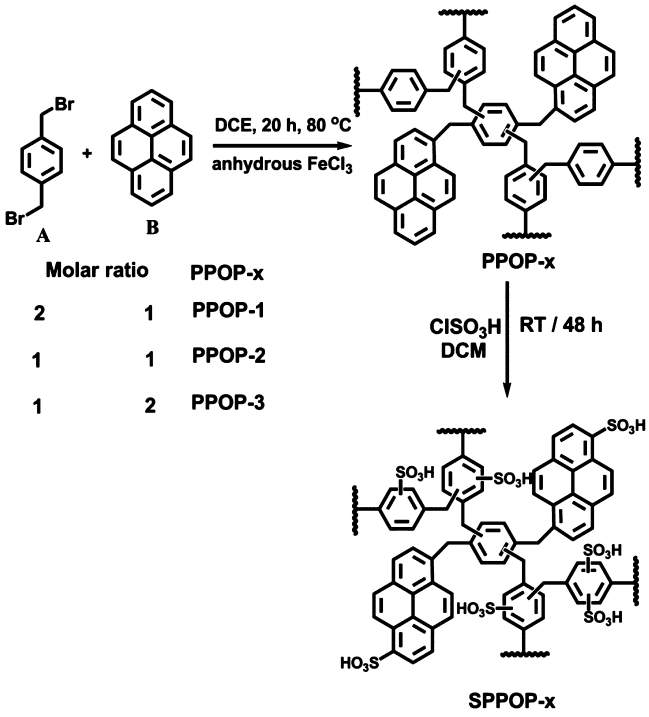

PPOP-2 and PPOP-3 were prepared by keeping the molar ratio of bis(1,4-bromomethyl)benzene and pyrene at 1:1 and 1:2, respectively.

Sulfonation of Porous Organic Polymers. PPOP-1, PPOP-2, and PPOP-3 were sulfonated following the literature procedure.[60] In a typical synthesis, 0.46 g of PPOP-1 taken in 10 mL dry dichloromethane was cooled in an ice-bath. A total of 9.2 mL of chlorosulfonic acid taken in 10 mL dry dichloromethane was added dropwise to the PPOP-1 suspension, and it was stirred at room temperature for 48 h. Then the mixture was poured into ice, and the solid was collected, washed with distilled water substantially, and dried to obtain SPPOP-1. PPOP-2 and PPOP-3 were sulfonated following a similar procedure to obtain SPPOP-2 and SPPOP-3, respectively. The outline for the synthesis of the organocatalyst SPPOP-1, SPPOP-2, and SPPOP-3 is shown in Scheme 1.

Procedure of Esterification and Transesterification Reactions. For esterification reactions, 1.0 mmol of a long chain fatty acid, 1.6 g of methanol, and the required amount of acid catalyst were mixed in a 25 mL round-bottom flask and stirred for 10 h at room temperature. Transesterification reactions were carried out by mixing 1 mmol of ethyl esters, 1.6 g of methanol, and the required amount of acid catalyst in a 25 mL round-bottom flask 24 h at room temperature. For the transesterification of vegetable oil, 100 mg of oil, 5 g of methanol, and the required amount of acid catalyst were mixed and stirred for 10 h at 298 and 333 K (Table 4). After completion of the reaction, the reaction mixture was filtered to separate the catalyst, and it was washed with 5 mL methanol. Then excess methanol was evaporated under reduced pressure to get isolated products, and the products were characterized by ^1H and ^{13}C NMR spectroscopy. The outline of esterification of fatty acids and transesterification of esters is shown in Scheme 2.

Reusability of Catalyst. In order to evaluate reusability of the catalyst, the catalyst is separated from the reaction mixture by filtration after completion of the reaction, and it has been thoroughly washed with methanol and acetone several times to remove any compounds that were adsorbed at the surface of the catalyst. Then the catalyst is dried overnight at 353 K before carrying out the next catalytic cycle. In this way, the esterification of lauric acid has been carried out six times, and reusability also has been tested for the esterification reaction of lauric acid in the presence of soybean oil at room temperature (298 K)

DOI: 10.1021/acssuschemeng.5b00238
ACS Sustainable Chem. Eng. 2015, 3, 1715−1723

Scheme 2. Esterification of Fatty Acids and Transesterification of Esters

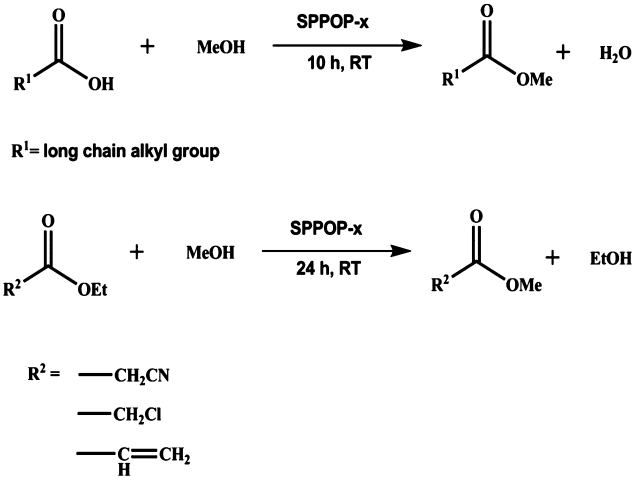

and also the transesterification reaction of soybean oil of the SPPOP-3 catalyst at 333 K. For both of these cases, we have carried out four reaction cycles and observed that the catalyst has nicely retained its catalytic activity.

Characterization Technique. Powder X-ray diffraction patterns were recorded on a Bruker D-8 advance SWAX diffractometer operated at 40 kV voltage and 40 mA current. The instrument has been calibrated with a standard silicon sample, using Ni-filtered Cu Kα (λ = 0.15406 nm) radiation. N_2 adsorption−desorption isotherms of polymer materials were obtained by using Quantachrome Autosorb-1C at 77 K. Prior to the gas adsorption studies, the samples were degassed at 423 K under high vacuum condition for 8 h. High resolution transmission electron microscopy (HR-TEM) images of the polymer samples were taken by using a JEOL JEM 2010 transmission electron microscope operating at 200 kV. A JEOL JEM 6700F field emission scanning electron microscope was used for the determination of the morphology the polymers. FT-IR spectra of the polymers were recorded using a PerkinElmer Spectrum 100. Thermogravimetric analysis (TGA) and differential thermal analysis (DTA) of the materials were determined in a TGA instrument thermal analyzer TA-SDT Q-600 under continuous flow of nitrogen with a heating/cooling rate 10 °C min^{-1}. Temperature-programmed desorption of ammonia (NH_3-TPD) was carried out in a Micromeritics ChemiSorb 2720. UV−visible diffuse reflectance spectra were recorded on a Shimadzu UV 2401PC with an integrating sphere attachment. $BaSO_4$ was used as the background standard. ^1H and ^{13}C NMR (solution) experiments were carried out on a Bruker DPX-400/500 spectrometer. The solid state MAS-NMR spectra of the samples were taken in Bruker Ascend 400 spectrometer.

RESULTS AND DISCUSSION

Wide angle powder X-ray diffraction of all the materials did not show any significant diffraction pattern and showed only very broad peaks (Figure S1, Supporting Information) suggesting the amorphous nature of cross-linked polymers. Surface porosity of PPOP-1 and SPPOP-1 materials is studied by BET analysis at 77 K using nitrogen as the sorbate molecule. This N_2 sorption analysis exhibits very high Brunauer−Emmett−Teller (BET) surface areas for PPOP-1 and SPPOP-1 of about 615 (Figure 1A) and 280 m^2g^{-1} (Figure 1B), respectively. Those N_2 sorption isotherms show combination of type I (sharp N_2 uptake at low P/Po) and IV (gradual increase in N_2 uptake at higher P/Po) according to IUPAC classification[61] with a broad hysteresis upon desorption.[62] Pore size distribution of PPOP-1 using the carbon slit pore model at 77 K determined by nonlocal density functional

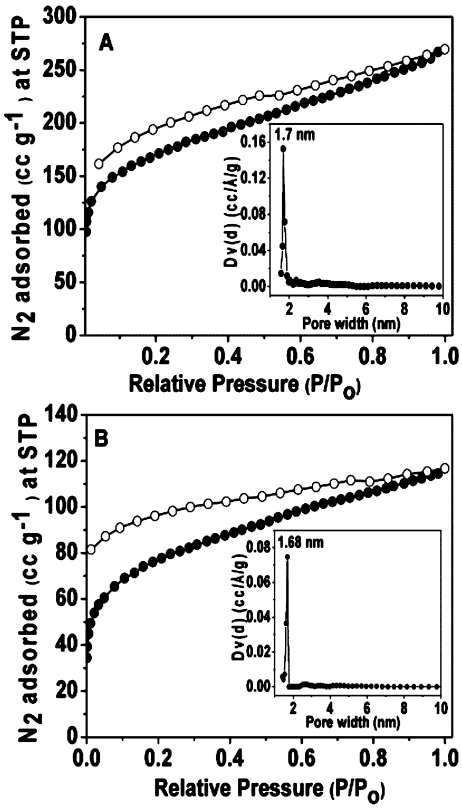

Figure 1. N_2 adsorption/desorption isotherm and pore size distribution (shown in inset) calculated from NLDFT method of PPOP-1 (A) and that of SPPOP-1 (B). Filled circles represent adsorption points, and empty circles represent desorption points.

theory (NLDFT) exhibited a dominant pore width centered at about 1.7 nm and that of SPPOP-1 centered at 1.68 nm (insets of Figures 1A,B). These pore size distribution results suggested the presence of supermicropores in these porous organic polymers. The micropore volume and the micropore surface area were determined by the t-method. The micropore volume and the micropore surface area of PPOP-1 are 0.2358 ccg^{-1} and 455 m^2g^{-1}, respectively. The total pore volume of PPOP-1 is 0.4179 ccg^{-1}, whereas the total pore volume of SPPOP-1 is 0.1810 ccg^{-1}. We have also studied surface porosity and pore size distribution of PPOP-2 and PPOP-3 and SPPOP-2 and SPPOP-3 materials (Table S1, Figures S2 and S3, Supporting Information).

The TEM images of PPOP-1 (Figure 2A,B) show nanofiber-like morphology having widths in the range of 80−120 nm and the length of the fiber of about 5 μm. Figure 2C and D show the corresponding TEM images of the sulfonated polymer SPPOP-1, which illustrates that the nanofiber morphology of the polymer has been retained after sulfonation. On the other hand, the TEM images of sulfonated polymer SPPOP-3 (Figure S4, Supporting Information) display spherical morphology having diameters in the range 0.5−1.2 μm. FE-SEM images of PPOP-1 and SPPOP-1 are shown in Figure 3. The SEM image of PPOP-1 (Figure 3A) further suggests cross-linked nanofiber morphology, whose width moderately increased upon sulfonation in SPPOP-1 (Figure 3B). FE-SEM images of PPOP-2, SPPOP-2, PPOP-3, and SPPOP-3 are shown in Figure S5 of the Supporting Information. From these images, it is clear that the nanofiber-like particle morphology of the polymers changed to spherical nanoparticles after sulfonation of the polymers.

DOI: 10.1021/acssuschemeng.5b00238
ACS Sustainable Chem. Eng. 2015, 3, 1715−1723

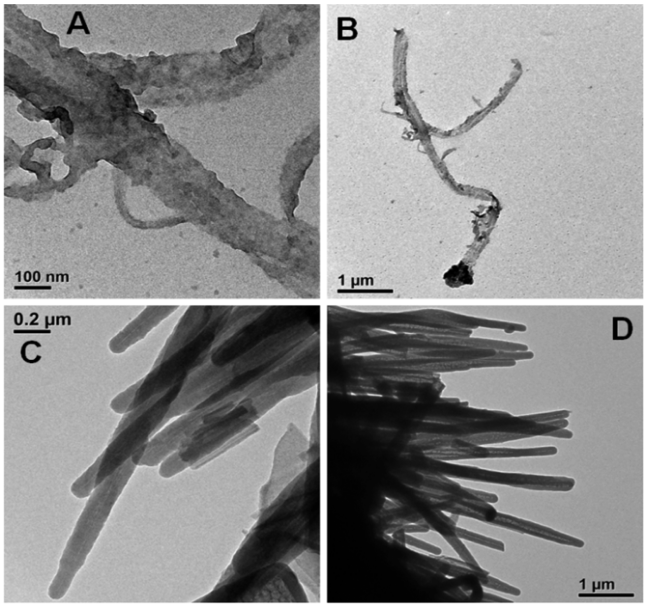

Figure 2. HR TEM images of PPOP-1 (A) and (B) and HR-TEM images of SPPOP-1 (C) and (D).

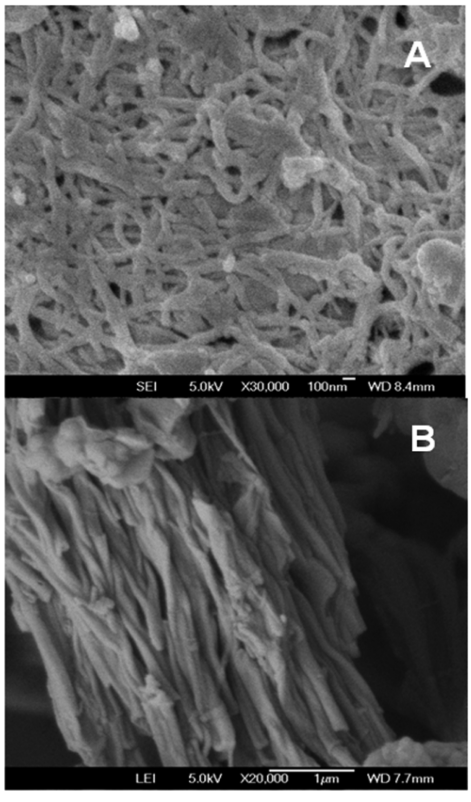

Figure 3. FE-SEM images of PPOP-1 (A) and SPPOP-1 (B).

The solid state ^{13}C CP MAS-NMR spectrum of PPOP-1 is shown in the Figure 4, which exhibits several signals at 136.06, 127.60, 54.90, and 36.50 ppm. Signals at 54.90 and 36.50 are attributed to benzyl carbon, and signals at 136.06 and 127.60 could be assigned to the carbon atoms of the benzene and pyrene rings. Further, the UV−vis absorption and photoluminescence spectra of PPOP-1 (Figure S6, Supporting Information) suggests the presence of pyrene rings in the porous polymeric framework.

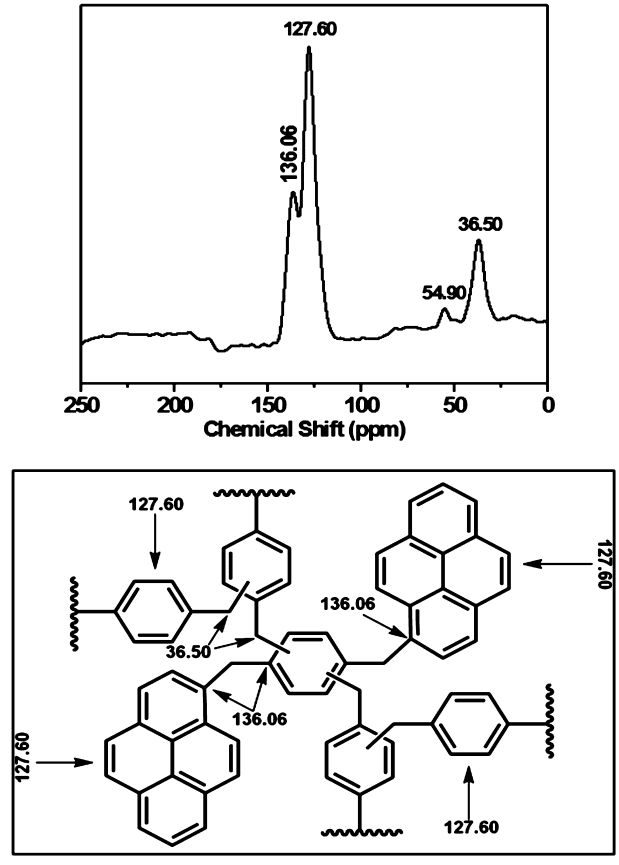

Figure 4. ^{13}C MAS-NMR spectrum of the PPOP-1.

Thermogravimetric (TG) analysis suggested high thermal stability of PPOP-1 and SPPOP-1 (Figure 5A and B, respectively). From the TGA plot of PPOP-1, it is shown that only 7% weight loss is observed up to 300 °C, and in the

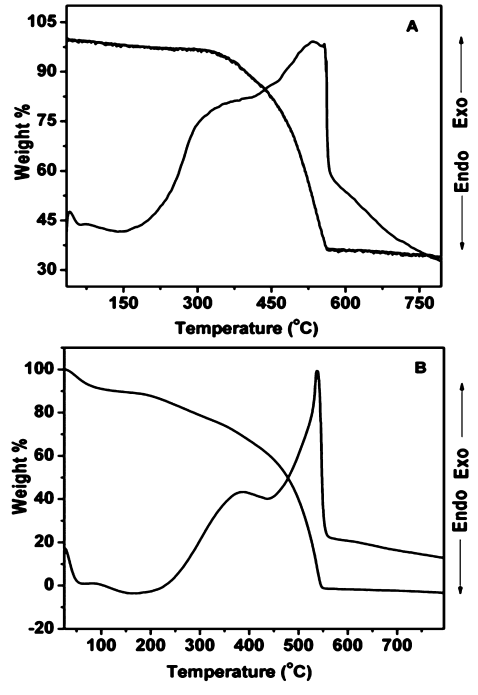

Figure 5. TG-DTA profiles of PPOP-1 (A) and SPPOP-1 (B).

DOI: 10.1021/acssuschemeng.5b00238
ACS Sustainable Chem. Eng. 2015, 3, 1715−1723

temperature range of 300 to 545 °C, sharp decrease in weight of about 52% is shown. The latter weight loss could be due to cleavage of C−C bonds present in the polymeric framework. This weight loss has been evidenced from the appearance of the long exothermic nature of the differential thermal analysis (DTA) plot. On the other hand, the TGA plot of SPPOP-1 shows about 25% weight loss up to 250 °C. In the temperature range of 250−537 °C, a sharp decrease in weight of about 68% is shown due to decomposition of the organic framework of the material. We also carried out thermogravimetric analysis on SPPOP-2 and SPPOP-3 in order to check their thermal stability (Figure S7A and S7B, Supporting Information, respectively).

NH_3-TPD analyses of the sulfonated materials are carried out to understand the nature and strength of the acid sites. In NH_3-TPD analysis, we have taken the desorption data of the volume of ammonia up to 250 °C of the TGA plot of SPPOP-1 to suggest this material almost retains its thermal stability up to this temperature. Volumes of ammonia desorbed correspond to 29.7 and 18.6 mL g^{-1} in the temperature ranges of 30−150 °C and 182−250 °C at STP for SPPOP-1 (Figure 6). These could

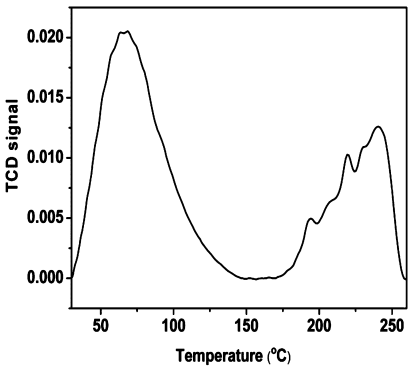

Figure 6. NH_3-TPD spectra of SPPOP-1.

be assigned to the weak and moderately strong Brønsted acid sites, respectively. Thus, NH_3-TPD results suggested a total of 2.15 mmol g^{-1} of Brønsted acidic sites present in the sulfonated porous polymer material SPPOP-1. We also carried out NH_3-TPD analysis on SPPOP-2 and SPPOP3 (Table 1, Figures S8 and S9, Supporting Information). The NH_3-TPD results suggested 2.82 and 3.22 mmol g^{-1} of Brønsted acidic sites present in SPPOP-2 and SPPOP-3 polymer material, respectively. Owing to the presence of these acid sites, these porous polymer materials could be employed as a heterogeneous catalyst in the esterification of long chain fatty acids and transesterification with methanol. Further, we have calculated the degree of sulfonation (% of sulfonation with respect to the total aromatic rings present) of sulfonated materials SPPOP-1, SPPOP-2, and SPPOP-3. The degree of sulfonation of SPPOP-1, SPPOP-2, and SPPOP-3 is 30%, 39%, and 44%, respectively, suggesting that with the increase in pyrene concentration the degree of sulfonation increases.

Table 1. Physico-Chemical Properties of Sulfonated Pyrene-Based Porous Organic Polymers

sulfonated catalyst	bis(1,4-bromomethyl) benzene: pyrene (molar ratio)	Brønsted acidic sites (mmol g^{-1})	degree of sulfonation (%)	BET surface area (m^2 g^{-1})
SPPOP-1	2:1	2.15	30	280
SPPOP-2	1:1	2.82	39	244
SPPOP-3	1:2	3.22	44	205

FT-IR spectra of PPOP-1, SPPOP-1, and reused SPPOP-1 materials are shown in Figure 7. In these spectra, absence of

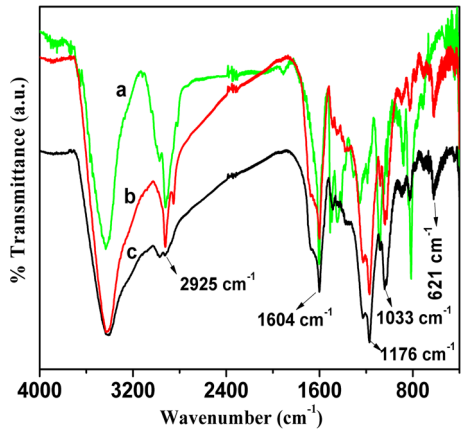

Figure 7. FT-IR spectra of PPOP-1 (a), sulfonated acid catalyst, SPPOP-1 (b), and reused catalyst, SPPOP-1 (c) after four cycles.

C−Br stretching clearly confirms the formation of a cross-linked polymer network. The bands around at 1604 and 2925 cm^{-1} could be assigned for aromatic C=C and sp^3 C−H bonds, respectively. The absorption peak for the C−H bending of the aromatic ring is observed at 816 cm^{-1}. Incorporation of $-SO_3H$ groups in the PPOP-1 network is confirmed by the FT-IR spectra of SPPOP-1. Compared with PPOP-1 in the FT-IR spectrum of SPPOP-1, new bands around at 621, 1033, and 1176 cm^{-1} are observed. These could be attributed to C−S stretching[63] and symmetric and asymmetric stretching of O=S=O[64] bonds, respectively. As shown in Figure S10 of the Supporting Information, the incorporation of $-SO_3H$ groups in the PPOP-2 and PPOP-3 network is also confirmed by FT-IR spectra of SPPOP-2 and SPPOP-3. Elemental analysis of fresh SPPOP-1 catalyst gave 54.40% carbon, 3.67% hydrogen, and 5.42% sulfur and that of reused SPPOP-1 after five reaction cycles gave 61.13% carbon, 5.07% hydrogen, and 4.50% sulfur. Increase in carbon content could be attributed to coke formation as usually encountered by the acid catalysts during prolonged catalytic runs. Similarly, elemental analysis shows that SPPOP-2 contains 57.32% carbon, 5.27% hydrogen, and 8.37% sulfur, and SPPOP-3 contains 58.73% carbon, 6.52% hydrogen, and 9.85% sulfur. We have calculated the degree of sulfonation on the basis of weight % of sulfur obtained from elemental analysis. The degree of sulfonation of SPPOP-1, SPPOP-2, and SPPOP-3 is 23%, 36%, and 42%, respectively, which agrees well with the result obtained independently from NH_3-TPD analysis.

SPPOP-1, SPPOP-2, and SPPOP-3 are employed as catalyst for the preparation of methyl esters of various long chain mono- and dicarboxylic fatty acids and transesterification of different ethyl esters, soybean, and olive oils, which are widely used as feedstock for the synthesis of biodiesels. The yields of these esterification reactions are given in Table 2. The results of the transesterification of esters are shown in Table 3, whereas the results of the transesterification of soybean and olive oils are given in Table 4. Usually esterification of free fatty acids (FFAs) is carried out at high temperature using the hazardous H_2SO_4 catalyst[65] where the separation of homogeneous catalyst[66] from the reaction mixture is a very difficult process. Several porous

DOI: 10.1021/acssuschemeng.5b00238
ACS Sustainable Chem. Eng. 2015, 3, 1715−1723

Table 2. Esterification Reactions of Various Long Chain Fatty Acids over Sulfonated Porous Polymers[a]

entry	fatty acid	catalyst	yield[b] (%)	TON[c]
1	$CH_3(CH_2)_{10}COOH$	SPPOP-1	90	16.7
2	$CH_3(CH_2)_{12}COOH$	SPPOP-1	89	16.5
3	$CH_3(CH_2)_{14}COOH$	SPPOP-1	90	16.7
4	$CH_3(CH_2)_{16}COOH$	SPPOP-1	92	17.1
5	$CH_3(CH_2)_7CH{=}CH(CH_2)_7COOH$	SPPOP-1	90	16.7
6	HOOC-$(CH_2)_8$-COOH	SPPOP-1	88	16.4
7	HOOC-$(CH_2)_3$-COOH	SPPOP-1	92	17.1
8	HOOC-$(CH_2)_4$-COOH	SPPOP-1	93	17.3
9[d]	$CH_3(CH_2)_{10}COOH$	no catalyst	8	-
10	$CH_3(CH_2)_{10}COOH$ in presence of soybean oil	SPPOP-1	88	16.4
11	$CH_3(CH_2)_{10}COOH$	SPPOP-2	91	16.9
12	$CH_3(CH_2)_{10}COOH$	SPPOP-3	94	17.5
13	$CH_3(CH_2)_7CH{=}CH(CH_2)_7COOH$	SPPOP-3	92	17.1
14[e]	$CH_3(CH_2)_{10}COOH$	Amberlite IR-120(H) resin	19	1.1

[a]Reaction conditions: 1 mmol of fatty acid, 1.6 g of methanol, 25 mg of SPPOP-1 or 19 mg of SPPOP-2 or 17 mg of SPPOP-3 (all contain 0.05375 mmol sulfonic groups) at room temperature (298 K); reaction time = 10 h. [b]Yield (%) was calculated from ^{1}H NMR: [peak area of one proton near 3.6 (for $-CH_3$) divided by that of one proton at 2.25 (for $-CH_2$)] × 100. [c]Turn over number (TON) = moles of substrate converted per mole of active site. [d]Reaction was carried out in the absence of any catalyst. [e]Reaction condition: 1 mmol of lauric acid, 100 mg of Amberlite IR-120(H) resin and its total exchange capacity = 1.8 mmol g^{-1} at room temperature (298 K); reaction time = 10 h. For all cases, the molar ratio of acid and methanol = 1:50.

Table 3. Transesterification reactions of different esters over sulfonated porous polymers[a]

entry	ester	catalyst	yield (%)	TON[b]
1	ethyl cyanoacetate	SPPOP-1	74	13.8
2	ethyl chloroacetate	SPPOP-1	45	8.4
3	ethyl acrylate	SPPOP-1	34	6.3
4	ethyl cyanoacetate	SPPOP-2	75	14.0
5	ethyl cyanoacetate	SPPOP-3	76	14.1
6[c]	ethyl cyanoacetate	Amberlite IR-120(H) resin	12	0.7

[a]Reaction conditions: 1 mmol of ester, 1.6 g of methanol, 25 mg of SPPOP-1 or 19 mg of SPPOP-2 or 17 mg of SPPOP-3 (all contain same mmol sulfonic groups) at room temperature (298 K); reaction time = 24 h. [b]Turn over number (TON) = moles of substrate converted per mole of active site. [c]Reaction condition: 1 mmol of ester, 100 mg of Amberlite IR-120(H) resin at room temperature (298 K); reaction time = 24 h. For all cases, the molar ratio of ester and methanol = 1:50.

Table 4. Transesterification of Soybean and Olive Oils over Sulfonated Porous Polymers[a]

entry	oil	catalyst	temperature (°c)	conversion (%)[b]
1	soybean oil	SPPOP-1	25	15
2	soybean oil	SPPOP-1	60	66
3	soybean oil	SPPOP-2	25	21.7
4	soybean oil	SPPOP-2	60	91.9
5	soybean oil	SPPOP-3	25	33.5
6	soybean oil	SPPOP-3	60	92.3
7	olive oil	SPPOP-1	25	19.5
8	olive oil	SPPOP-1	60	48
9	olive oil	SPPOP-2	25	27.7
10	olive oil	SPPOP-2	60	85.9
11	olive oil	SPPOP-3	25	31.3
12	olive oil	SPPOP-3	60	93.8
13[c]	soybean oil	Amberlite IR-120(H) resin	25	no reaction
14[c]	soybean oil	Amberlite IR-120(H) resin	60	3.4

[a]Reaction conditions: 100 mg of soybean oil or 100 mg of olive oil, 5 g of methanol, and 25 mg of SPPOP-1 or 19 mg of SPPOP-2 or 17 mg of SPPOP-3 (all contain same mmol sulfonic groups); reaction time = 10 h. [b]Conversion (%) was calculated from integration values of the glyceridic and methyl ester protons in ^{1}H NMR by the equation:

$$\text{Conversion} = \frac{5 \times I_{ME}}{(5 \times I_{ME}) + (9 \times I_{TG})} \times 100\%$$

I_{ME} is the integration value of the methyl ester peak, and I_{TG} is the integration value of the glyceridic peaks in the triglycerides of oil. [c]100 mg of Amberlite IR-120(H) resin was taken.

solid acid catalysts have been reported for the production of biofuels.[67] But most of the reactions are carried out at high temperature.[68] There are very recent reports on porous sulfonated zinc phosphonate[69] and tin(IV) phosphonate materials[70] for the synthesis of biodiesels, where the reactions are carried out at room temperature (298 and 323 K, respectively). But the present catalytic pathway for biodiesel production is unique and green as the reactions proceed at room temperature over a metal-free organocatalyst. It is shown from the tables that the product yield increases from SPPOP-1 to SPPOP-2 and then to SPPOP-3. Total acidity of these materials also increases in this order. Thus, we can conclude that due to the presence of higher Brønsted acidic sites, the SPPOP-3 catalyst shows higher catalytic activity than the SPPOP-1 and SPPOP-2 materials.

Mainly three reaction parameters, i.e., reaction time, temperature, and molar ratio of fatty acid to methanol, influence the conversion of fatty acids to biofuels. Here, we have carried out the reactions at room temperature (298 K). It takes about 10 h time to complete the reactions for most of the substrates. The reaction time is an important parameter for these esterification reactions. Figure 8 shows the conversion of fatty acids to corresponding esters gradually increasing with time. We have examined that if we have carried out the reaction (studied taking lauric acid as reference) at higher temperature, i.e., 313 and 333 K, it requires much less reaction time (5 h when reaction has been carried out at 313 K and 4 h when

DOI: 10.1021/acssuschemeng.5b00238
ACS Sustainable Chem. Eng. 2015, 3, 1715−1723

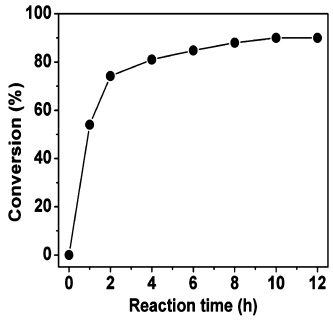

Figure 8. Reaction time vs conversion (%) curve for lauric acid at room temperature.

reaction has been carried out at 333 K temperature) to achieve the same yield as that obtained at room temperature. These esterification reactions are reversible in nature. At the initial stage, the rate of forward reaction is much higher than that of the reverse reaction because of high concentration of the reactants and low concentration of the product. The molar ratio of fatty acid to methanol is an important parameter for the conversion of fatty acids to biofuels. Theoretically, one mole fatty acid needs one mole of methanol to get converted into the corresponding methyl ester. Because of the reversible reaction, we have shown that the excess of methanol relative to fatty acid can shift the equilibrium toward methyl ester formation.[71] The yield of methyl esters gets increased from 70% to 90% after 10 h of reaction with an increase in molar ratio of fatty acid to methanol from 1:5 to 1:50. Here, excess methanol is used to move the reaction toward the forward direction with higher yield.

To test the reusability of the sulfonated polymer catalyst, we have carried out the esterification of lauric acid for six consecutive reaction cycles. The detailed kinetics (conversion vs time plots) of this catalytic esterification is shown in Figure 9. As shown from the plot, progress of the reaction at different

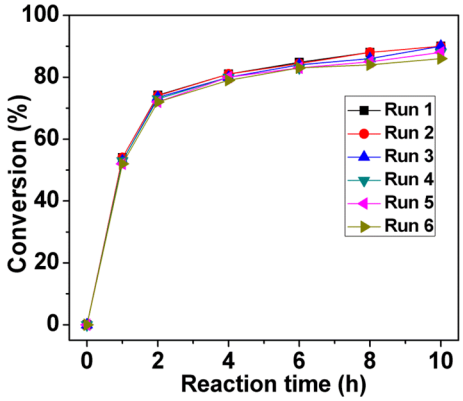

Figure 9. Recyclability of SPPOP-1 catalyst in the esterification of lauric acid.

reaction hours proceeds in a similar fashion, and the sulfonated porous polymer SPPOP-1 has retained its catalytic activity over several reaction cycles efficiently. This result suggests that the pyrene-based sulfonated porous polymers can be employed efficiently for several solid acid catalyzed reactions.

Leaching Test. The heterogeneity of the catalyst was verified by a leaching test. In the esterification reaction of lauric acid, the catalyst is separated out from the reaction mixture after 1.5 h through filtration, and at that time, the yield of ester was 64%. Then the reaction is continued for 8.5 h at room temperature without catalyst. After 10 h, the yield was just increased to 67%. This result confirms that during the reaction no leaching of sulfonate group takes place. We have carried out the esterification reaction of lauric acid in the presence of soybean oil at 298 K and the transesterification reaction of soybean oil at 333 K over SPPOP-3 for testing whether the catalyst is leached out or not during the reaction medium. We have followed the same procedure for both reactions. NH_3-TPD results of the used SPPOP-3 after these reactions suggested almost no change in total acidity of the material. This result suggested that our sulfonated porous polymers are stable, and no leaching of the $-SO_3H$ group took place during the liquid phase esterification and transesterification reactions.

CONCLUSIONS

We have designed three new pyrene-based porous organic polymers via Friedel–Crafts alkylation of pyrene and bis(1,4-dibromomethyl)benzene in different molar ratios by using $FeCl_3$ catalyst in dichloroethane solvent under refluxing conditions. These porous polymers are sulfonated to obtain microporous-sulfonated pyrene-based organic frameworks, SPPOP-1, SPPOP-2, and SPPOP-3, consisting of different molar ratios of pyrene and bis(1,4-dibromomethyl)benzene. These nontoxic and eco-friendly sulfonated materials have been employed as efficient heterogeneous strong acid catalysts for the synthesis of biodiesels from different long chain fatty acids and transesterification reactions of different ethyl esters and vegetable oils. The catalytic activity increases with the degree of sulfonation. Among the three acid catalysts, SPPOP-3 bearing the highest degree of sulfonation exhibits the best catalytic activity. In addition, the stability and catalytic activity of the sulfonated catalyst has been retained after several successive reaction cycles without leaching of the functional groups, suggesting a sustainable future for these pyrene-based porous polymers in solid acid catalysis.

ASSOCIATED CONTENT

Supporting Information

Wide angle powder XRD pattern, N_2 adsorption–desorption isotherm, HR-TEM, FE-SEM, NH_3-TPD, UV-visible absorption and photoluminescence spectra, and ^1H and ^{13}C NMR spectra. The Supporting Information is available free of charge on the ACS Publications website at DOI: 10.1021/acssuschemeng.5b00238.

AUTHOR INFORMATION

Corresponding Author

*E-mail: msab@iacs.res.in. Tel: 91-33-2473-4971. Fax: 91-33-2473-2805.

Notes

The authors declare no competing financial interest.

ACKNOWLEDGMENTS

S.K.K. thanks CSIR, New Delhi, for providing a senior research fellowship to him. A.B. thanks DST, New Delhi, for providing instrumental facility through the DST unit on Nanoscience and DST-SERB project grants.

DOI: 10.1021/acssuschemeng.5b00238
ACS Sustainable Chem. Eng. 2015, 3, 1715–1723

REFERENCES

(1) Berchmans, H. J.; Hirata, S. Biodiesel Production from Crude Jatropha Curcas L. Seed Oil with a High Content of Free Fatty Acids. *Bioresour. Technol.* **2008**, *99*, 1716−1721.

(2) Demirbas, A. Progress and Recent Trends in Biodiesel Fuels. *Energy Convers. Manage.* **2009**, *50*, 14−34.

(3) Lotero, E.; Liu, Y.; Lopez, D. E.; Suwannakarn, K.; Bruce, D. A.; Goodwin, J. G., Jr. Synthesis of Biodiesel via Acid Catalysis. *Ind. Eng. Chem. Res.* **2005**, *44*, 5353−5363.

(4) Leung, D. Y. C.; Wu, X.; Leung, M. K. H. A Review on Biodiesel Production using Catalyzed Transesterification. *Appl. Energy* **2010**, *87*, 1083−1095.

(5) Climent, M. J.; Corma, A.; Iborra, S. Conversion of Biomass Platform Molecules into Fuel Additives and Liquid Hydrocarbon Fuels. *Green Chem.* **2014**, *16*, 516−547.

(6) Boffito, D. C.; Mansi, S.; Leveque, J.-M.; Pirola, C.; Bianchi, C. L.; Patience, G. S. Ultrafast Biodiesel Production Using Ultrasound in Batch and Continuous Reactors. *ACS Sustainable Chem. Eng.* **2013**, *1*, 1432−1439.

(7) Veljković, V. B.; Stamenković, O. S.; Tasić, M. B. The Wastewater Treatment in the Biodiesel Production with Alkali-Catalyzed Transesterification. *Renewable Sustainable Energy Rev.* **2014**, *32*, 40−60.

(8) Dinjus, E.; Arnold, U.; Dahmen, N.; Höfer, R.; Wach, W. *Sustainable Solutions for Modern Economies*; RSC Green Chemistry Series; Höfer, R., Ed.; RSC Publishing: Cambridge, 2009; Volume 4, pp 125−163.

(9) Galhardo, T. S.; Simone, N.; Goncalves, M.; Figueiredo, F. C. A.; Mandelli, D.; Carvalho, W. A. Preparation of Sulfonated Carbons from Rice Husk and Their Application in Catalytic Conversion of Glycerol. *ACS Sustainable Chem. Eng.* **2013**, *1*, 1381−1389.

(10) Marchetti, J. M.; Errazu, A. F. Esterification of Free Fatty Acids using Sulfuric Acid as Catalyst in the Presence of Triglycerides. *Biomass Bioenergy* **2008**, *32*, 892−895.

(11) Aranda, D. A. G.; Santos, R. T. P.; Tapanes, N. C. O.; Ramos, A. L. D.; Antunes, O. A. C. Acid-Catalyzed Homogeneous Esterification Reaction for Biodiesel Production from Palm Fatty Acids. *Catal. Lett.* **2008**, *122*, 20−25.

(12) Knothe, G.; Dunn, R. O.; Bagby, M. O. Biodiesel: The Use of Vegetable Oils and Their Derivatives as Alternative Diesel Fuels. In *Fuels and Chemicals from Biomass*; Saha, B. C., Woodward, J., Eds.; ACS Symposium Series 666; American Chemical Society; Washington, DC, 1997; Chapter 10.

(13) Kiss, A. A.; Dimian, A. C.; Rothenberg, G. Solid Acid Catalysts for Biodiesel Production - Towards Sustainable Energy. *Adv. Synth. Catal.* **2006**, *348*, 75−81.

(14) Bournay, L.; Casanave, D.; Delfort, B.; Hillion, G.; Chodorge, J. A. New Heterogeneous Process for Biodiesel Production: A Way to Improve the Quality and the Value of the Crude Glycerine Produced by Biodiesel Plants. *Catal. Today* **2005**, *106*, 190−192.

(15) Kinney, A. J.; Clemente, T. E. Modifying Soybean Oil for Enhanced Performance in Biodiesel Blends. *Fuel Process. Technol.* **2005**, *86*, 1137−1147.

(16) Felizardo, P.; Correia, M. J. N.; Raposo, I.; Mendes, J. F.; Berkemeier, R.; Bordado, J. M. Production of Biodiesel from Waste Frying Oils. *Waste Manage.* **2006**, *26*, 487−494.

(17) Kulkarni, M. G.; Dalai, A. K. Waste Cooking Oils an Economical Source for Biodiesel: a Review. *Ind. Eng. Chem. Res.* **2006**, *45*, 2901−2913.

(18) Canakci, M. The Potential of Restaurant Waste Lipids as Biodiesel Feedstocks. *Bioresour. Technol.* **2007**, *98*, 183−190.

(19) Yadav, G. D.; Nair, J. J. Sulfated Zirconia and Its Modified Versions as Promising Catalysts for Industrial Processes. *Microporous Mesoporous Mater.* **1999**, *33*, 1−48.

(20) Furuta, S.; Matsuhashi, H.; Arata, K. Biodiesel Fuel Production with Solid Superacid Catalysis in Fixed Bed Reactor under Atmospheric Pressure. *Catal. Commun.* **2004**, *5*, 721−723.

(21) Furuta, S.; Matsuhashi, H.; Arata, K. Catalytic Action of Sulfated Tin Oxide for Etherification and Esterification in Comparison with Sulfated Zirconia. *Appl. Catal., A* **2004**, *269*, 187−191.

(22) Liu, R.; Wang, X.; Zhao, X.; Feng, P. Sulfonated Ordered Mesoporous Carbon for Catalytic Preparation of Biodiesel. *Carbon* **2008**, *46*, 1664−1669.

(23) Mo, X.; Lotero, E.; Lu, C.; Liu, Y.; Goodwin, J. G. A Novel Sulfonated Carbon Composite Solid Acid Catalyst for Biodiesel Synthesis. *Catal. Lett.* **2008**, *123*, 1−6.

(24) Luque, R.; Clark, J. H. Biodiesel-Like Biofuels from Simultaneous Transesterification/Esterification of Waste Oils with a Biomass-Derived Solid Acid Catalyst. *ChemCatChem* **2011**, *3*, 594−597.

(25) Blagov, S.; Parada, S.; Bailer, O.; Moritz, P.; Lam, D.; Weinand, R.; Hasse, H. Influence of Ion-exchange Resin Catalysts on Side Reactions of the Esterification of n-Butanol with Acetic Acid. *Chem. Eng. Sci.* **2006**, *61*, 753−765.

(26) Ni, J.; Meunier, F. C. Esterification of Free Fatty Acids in Sunflower Oil over Solid Acid Catalysts using Batch and Fixed Bed-Reactors. *Appl. Catal., A* **2007**, *333*, 122−130.

(27) Toda, M.; Takagaki, A.; Okamura, M.; Kondo, J. N.; Hayashi, S.; Domen, K.; Hara, M. Biodiesel Made with Sugar Catalyst. *Nature* **2005**, *438*, 178.

(28) Okamura, M.; Takagaki, A.; Toda, M.; Kondo, J. N.; Domen, K.; Tatsumi, T.; Hara, M.; Hayashi, S. Acid-Catalyzed Reactions on Flexible Polycyclic Aromatic Carbon in Amorphous Carbon. *Chem. Mater.* **2006**, *18*, 3039−3045.

(29) Zong, M.-H.; Duan, Z.-Q.; Lou, W.-Y.; Smith, T. J.; Wu, H. Preparation of a Sugar Catalyst and Its Use for Highly Efficient Production of Biodiesel. *Green Chem.* **2007**, *9*, 434−437.

(30) Takagaki, A.; Toda, M.; Okamura, M.; Kondo, J. N.; Hayashi, S.; Domen, K.; Hara, M. Esterification of Higher Fatty Acids by a Novel Strong Solid Acid. *Catal. Today* **2006**, *116*, 157−161.

(31) Das, S. K.; Bhunia, M. K.; Sinha, A. K.; Bhaumik, A. Synthesis, Characterization, and Biofuel Application of Mesoporous Zirconium Oxophosphates. *ACS Catal.* **2011**, *1*, 493−501.

(32) Wee, L. H.; Bajpe, S. R.; Janssens, N.; Hermans, I.; Houthoofd, K.; Kirschhock, C. E. A.; Martens, J. A. Convenient Synthesis of $Cu_3(BTC)_2$ Encapsulated Keggin Heteropolyacid Nanomaterial for Application in Catalysis. *Chem. Commun.* **2010**, *46*, 8186−8188.

(33) Testa, M. L.; La Parola, V.; Venezia, A. M. Esterification of Acetic Acid with Butanol over Sulfonic Acid-Functionalized Hybrid Silicas. *Catal. Today* **2010**, *158*, 109−113.

(34) de Godoi Silva, V. W.; Laier, L. O.; Silva, M. J. d. Novel $H_3PW_{12}O_{40}$: Catalysed Esterification Reactions of Fatty Acids at Room Temperature for Biodiesel Production. *Catal. Lett.* **2010**, *135*, 207−211.

(35) Kosal, M. E.; Chou, J.-H.; Wilson, S. R.; Suslick, K. S. A Functional Zeolite Analogue Assembled from Metalloporphyrins. *Nat. Mater.* **2002**, *1*, 118−121.

(36) Thomas, A. Functional Materials: from Hard to Soft Porous Frameworks. *Angew. Chem., Int. Ed.* **2010**, *49*, 8328−8344.

(37) Kanoo, P.; Gurunatha, K. L.; Maji, T. K. Versatile Functionalities in MOFs Assembled from the Same Building Units: Interplay of Structural Flexibility, Rigidity and Regularity. *J. Mater. Chem.* **2010**, *20*, 1322−1331.

(38) Bae, Y.-S.; Farha, O. K.; Spokoyny, A. M.; Mirkin, C. A.; Hupp, J. T.; Snurr, R. Q. Carborane-Based Metal−organic Frameworks as Highly Selective Sorbents for CO_2 over Methane. *Chem. Commun.* **2008**, 4135−4137.

(39) Li, J.-R.; Kuppler, R. J.; Zhou, H.-C. Selective Gas Adsorption and Separation in Metal-organic Frameworks. *Chem. Soc. Rev.* **2009**, *38*, 1477−1504.

(40) Xue, Z.; Sun, Z.; Cao, Y.; Chen, Y.; Tao, L.; Li, K.; Feng, L.; Fu, Q.; Wei, Y. Superoleophilic and Superhydrophobic Biodegradable Material with Porous Structures for Oil Absorption and Oil-Water Separation. *RSC Adv.* **2013**, *3*, 23432−23437.

(41) Patel, H. A.; Je, S. H.; Park, J.; Jung, Y.; Coskun, A.; Yavuz, C. T. Directing the Structural Features of N_2-Phobic Nanoporous Covalent Organic Polymers for CO_2 Capture and Separation. *Chem. - Eur. J.* **2014**, *20*, 772−780.

DOI: 10.1021/acssuschemeng.5b00238
ACS Sustainable Chem. Eng. 2015, 3, 1715−1723

(42) Ren, S.; Bojdys, M. J.; Dawson, R.; Laybourn, A.; Khimyak, Y. Z.; Adams, D. J.; Cooper, A. I. Porous, Fluorescent, Covalent Triazine-Based Frameworks via Room-Temperature and Microwave-Assisted Synthesis. *Adv. Mater.* **2012**, *24*, 2357−2361.
(43) Kang, N.; Park, J. H.; Ko, K. C.; Chun, J.; Kim, E.; Shin, H. W.; Lee, S. M.; Kim, H. J.; Ahn, T. K.; Lee, J. Y.; Son, S. U. Tandem Synthesis of Photoactive Benzodifuran Moieties in the Formation of Microporous Organic Networks. *Angew. Chem., Int. Ed.* **2013**, *52*, 6228−6232.
(44) Modak, A.; Nandi, M.; Mondal, J.; Bhaumik, A. Porphyrin Based Porous Organic Polymers: Novel Synthetic Strategy and Exceptionally High CO_2 Adsorption Capacity. *Chem. Commun.* **2012**, *48*, 248−250.
(45) Chaikittisilp, W.; Ariga, K.; Yamauchi, Y. A New Family of Carbon Materials: Synthesis of MOF-Derived Nanoporous Carbons and Their Promising Applications. *J. Mater. Chem. A* **2013**, *1*, 14−19.
(46) Furukawa, H.; Yaghi, O. M. Storage of Hydrogen, Methane, and Carbon Dioxide in Highly Porous Covalent Organic Frameworks for Clean Energy Applications. *J. Am. Chem. Soc.* **2009**, *131*, 8875−8883.
(47) Rosi, N. L.; Eckert, J.; Eddaoudi, M.; Vodak, D. T.; Kim, J.; O'Keeffe, M.; Yaghi, O. M. Hydrogen Storage in Microporous Metal-Organic Frameworks. *Science* **2003**, *300*, 1127−1129.
(48) Martin, R. L.; Simon, C. M.; Smit, B.; Haranczyk, M. *J. Am. Chem. Soc.* **2014**, *136*, 5006−5022.
(49) Zhu, Y.; Murali, S.; Stoller, M. D.; Ganesh, K. J.; Cai, W.; Ferreira, P. J.; Pirkle, A.; Wallace, R. M.; Cychosz, K. A.; Thommes, M.; Su, D.; Stach, E. A.; Ruoff, R. S. Carbon-Based Supercapacitors Produced by Activation of Graphene. *Science* **2011**, *332*, 1537−1541.
(50) Liu, X. M.; Zhang, Y. W.; Li, H.; A, S.; Xia, H.; Mu, Y. Triarylboron-Based Fluorescent Conjugated Microporous Polymers. *RSC Adv.* **2013**, *3*, 21267−21270.
(51) Novotney, J. L.; Dichtel, W. R. Conjugated Porous Polymers for TNT Vapor Detection. *ACS Macro Lett.* **2013**, *2*, 423−426.
(52) Zhang, Y. W.; A, S.; Zou, Y. C.; Luo, X. L.; Li, Z. P.; Xia, H.; Liu, X. M.; Mu, Y. Gas Uptake, Molecular Sensing and Organocatalytic Performances of a Multifunctional Carbazole-Based Conjugated Microporous Polymer. *J. Mater. Chem. A* **2014**, *2*, 13422−13430.
(53) Kaur, P.; Hupp, J. T.; Nguyen, S. T. Porous Organic Polymers in Catalysis: Opportunities and Challenges. *ACS Catal.* **2011**, *1*, 819−835.
(54) Zhang, Y.; Riduan, S. N. Functional Porous Organic Polymers for Heterogeneous Catalysis. *Chem. Soc. Rev.* **2012**, *41*, 2083−2094.
(55) Modak, A.; Mondal, J.; Bhaumik, A. Highly Porous Organic Polymer Containing $-CO_2H$ Groups: A Convenient Carbocatalyst for Indole C-H Activation at Room Temperature. *ChemCatChem* **2013**, *5*, 1749−1753.
(56) Xu, X. M.; Cheng, T. Y.; Liu, X. C.; Xu, J. Y.; Jin, R. H.; Liu, G. H. Chiral Squaramide-Functionalized Imidazoliurn-Based Organic-Inorganic Hybrid Silica Promotes Asymmetric Michael Addition of 1,3-Dicarbonyls to Nitroalkenes in Brine. *ACS Catal.* **2014**, *4*, 2137−2142.
(57) Verde-Sesto, E.; Pintado-Sierra, M.; Corma, A.; Maya, E. M.; de la Campa, J. G.; Iglesias, M.; Sanchez, F. First Pre-Functionalised Polymeric Aromatic Framework from Mononitrotetrakis (iodophenyl)methane and Its Application. *Chem. - Eur. J.* **2014**, *20*, 5111−5120.
(58) Schmidt, J.; Kundu, D. S.; Blechert, S.; Thomas, A. Tuning Porosity and Activity of Microporous Polymer Network Organocatalysts by Co-polymerisation. *Chem. Commun.* **2014**, *50*, 3347−3349.
(59) Bhunia, S.; Banerjee, B.; Bhaumik, A. A New Hypercrosslinked Supermicroporous Polymer, with Scope for Sulfonation, and Its Catalytic Potential for the Efficient Synthesis of Biodiesel at Room Temperature. *Chem. Commun.* **2015**, *51*, 5020−5023.
(60) Lu, W.; Yuan, D.; Sculley, J.; Zhao, D.; Krishna, R.; Zhou, H.-C. Sulfonate-Grafted Porous Polymer Networks for Preferential CO_2 Adsorption at Low Pressure. *J. Am. Chem. Soc.* **2011**, *133*, 18126−18129.
(61) Patel, H. A.; Je, S. H.; Park, J.; Chen, D. P.; Jung, Y.; Yavuz, C. T.; Coskun, A. Unprecedented High-Temperature CO_2 Selectivity in N_2-Phobic Nanoporous Covalent Organic Polymers. *Nat. Commun.* **2013**, *4*, 1357.
(62) Makhseed, S.; Samuel, J. Microporous Organic Polymers Incorporating Dicarboximide Units for H_2 Storage and Remarkable CO_2 Capture. *J. Mater. Chem. A* **2013**, *1*, 13004−13010.
(63) Lou, W. Y.; Guo, Q.; Chen, W. J.; Zong, M. H.; Wu, H.; Smith, T. J. A Highly Active Bagasse-Derived Solid Acid Catalyst with Properties Suitable for Production of Biodiesel. *ChemSusChem* **2012**, *5*, 1533−1541.
(64) Suganuma, S.; Nakajima, K.; Kitano, M.; Hayashi, S.; Hara, M. sp^3-Linked Amorphous Carbon with Sulfonic Acid Groups as a Heterogeneous Acid Catalyst. *ChemSusChem* **2012**, *5*, 1841−1846.
(65) Bojan, S. G.; Durairaj, S. K. Producing Biodiesel from High Free Fatty Acid Jatropha Curcas Oil by a Two Step Method-an Indian Case Study. *J. Sustain. Ener. Environ.* **2012**, *3*, 63−66.
(66) Tariq, M.; Ali, S.; Khalid, N. Activity of Homogeneous and Heterogeneous Catalysts, Spectroscopic and Chromatographic Characterization of Biodiesel: A Review. *Renewable Sustainable Energy Rev.* **2012**, *16*, 6303−6316.
(67) Zabeti, M.; Wan Daud, W. M. A.; Aroua, M. K. Activity of Solid Catalysts for Biodiesel Production: A Review. *Fuel Process. Technol.* **2009**, *90*, 770−777.
(68) Granados, M. L.; Poves, M. D. Z.; Alonso, D. M.; Mariscal, R.; Galisteo, F. C.; Moreno-Tost, R.; Santamaria, J.; Fierro, J. L. G. Biodiesel from Sunflower Oil by using Activated Calcium Oxide. *Appl. Catal., B* **2007**, *73*, 317−326.
(69) Pramanik, M.; Nandi, M.; Uyama, H.; Bhaumik, A. Organic−inorganic Hybrid Porous Sulfonated Zinc Phosphonate Material: Efficient Catalyst for Biodiesel Synthesis at Room Temperature. *Green Chem.* **2012**, *14*, 2273−2281.
(70) Dutta, A.; Patra, A. K.; Uyama, H.; Bhaumik, A. Template-Free Synthesis of a Porous Organic-inorganic Hybrid Tin(IV) Phosphonate and Its High Catalytic Activity for Esterification of Free Fatty Acids. *ACS Appl. Mater. Interfaces* **2013**, *5*, 9913−9917.
(71) Lou, W. Y.; Zong, M. H.; Duan, Z. Q. Efficient Production of Biodiesel from High Free Fatty Acid-Containing Waste Oils using Various Carbohydrate-Derived Solid Acid Catalysts. *Bioresour. Technol.* **2008**, *99*, 8752−8758.

DOI: 10.1021/acssuschemeng.5b00238
ACS Sustainable Chem. Eng. 2015, 3, 1715−1723